Activated Carbon Production from Low Ash Subbituminous Coal with CO_2 Activation

Hsisheng Teng and Hung-Chi Lin
Dept. of Chemical Engineering, National Cheng Kung University, Tainan 70101, Taiwan

Activated carbon was prepared by physical activation in CO_2 from a low-ash subbituminous coal. The preparation process consisted of carbonization of the coal in N_2 followed by activation of the resulting chars in CO_2. The activation temperature ranged from 700 to 950°C. Experimental results revealed that the surface area, pore volume and average pore diameter of the activated carbon generally increased with the amount of carbon burnoff carried out at the same temperature. These surface characteristics were also influenced by the variation of the activation temperature. It was found that the porosity of the carbon passed through a maximum at a temperature of 750°C. The activation energy for the carbon gasification in CO_2 was calculated to be in a range of 130 – 180 kJ/mol, based on the assumption that the reaction rate was proportional to the surface area of the carbon. The apparent order with respect to CO_2 partial pressure for the gasification was found to be within the range of 0.15 – 0.25.

Introduction

Activated carbons, with their high porosity, are extensively used in industrial purification and chemical recovery operations. Various commercial activated carbons with different properties are manufactured for different applications. The source material and preparation process are the most important factors determining the properties of the carbons. Basically, almost any carbonaceous material can be converted into activated carbon (Muñoz-Guillena et al., 1992; Greenbank and Spotts, 1993). Nevertheless, the final properties of the carbon will reflect to a considerable extent the nature of the source material (Cooney, 1980). Most types of industrial activated carbons are produced from naturally occurring carbonaceous materials like coal, petroleum, peat, wood, and vegetable. Because of its availability and cheapness, coal is the most commonly used precursor for activated carbon production (Ahmadpour and Do, 1996; Muñoz-Guillena et al., 1992; Bansal et al., 1988).

The high adsorptive capacities of activated carbons are mainly associated with their internal pore properties such as surface area, pore volume, and pore-size distribution. Generally, activated carbons are mainly microporous, but in addition to micropores they contain meso- and macropores, which are very important in facilitating access of the adsorbate molecules to the interior of carbon particles (Ahmadpour and Do, 1995). Practically, the type of porosity is dictated by the type of raw material employed; however, the method of activation is another parameter that may influence the final pore-size distribution (Laine and Yunes, 1992).

In principle, there are two different processes for the preparation of activated carbon: physical and chemical. Comparing these two processes, physical activation is favored when the environmental contamination and equipment corrosion caused by the chemical agents are considered as important drawbacks for chemical activation processes. Physical activation was employed in the present study. Basically, preparation of activated carbon with physical activation involves carbonization of a carbonaceous precursor followed by burnoff of the resulting char in the presence of some mildly oxidizing gases such as carbon dioxide or steam (Bansal et al., 1988; Wigmans, 1989).

Coal with a low ash content is generally favored for preparing activated carbons from physical activation, since the ash has negligible specific surface area and pore volume compared to the microporous carbon. Its increasing presence with increasing carbon burnoff will increasingly contribute to reducing the measured surface area and pore volumes. Besides, in requiring the lower emission of sulfur oxides during carbon burnoff, coal with a low-sulfur content is preferred in

Correspondence concerning this article should be addressed to H. Teng.

activated-carbon production. Because of these considerations, a low-ash and low-sulfur subbituminous coal was chosen as a precursor of activated carbon in the present study.

In preparing activated carbons from coal with physical activation, the temperature for coal carbonization has been reported to have influence on the surface properties of the resulting carbons (Teng et al., 1996, 1997; Wigmans, 1989). The further activation, following the carbonization, is implemented to increase the surface area and pore volume of the carbon. Changes in surface area and pore volume during activation are often monitored and controlled to produce various activated carbons for different applications (Lu, 1994). Variations in surface area and pore volume with carbon burnoff during activation are normally taken as the essential characteristics of a particular activation process.

Within the preceding scope this study is devoted to the effects of different parameters on the preparation of activated carbon from the subbituminous coal with CO_2 activation. This article describes the influence of the preparation temperature on the properties of the resulting chars, the gasification kinetics during activation in CO_2, and the development of the surface structure of the carbon with the extent of carbon burnoff.

Experimental Section

Raw material

An Indonesian subbituminous coal, Adaro (AD), was used as the starting material. This coal is very low in both sulfur and ash contents. The proximate and ultimate analyses of the raw coal are shown in Table 1. The as-received coals were ground and sieved to a particle size of 210–300 μm before being treated.

Carbonization

Pyrolysis of the fresh coal was performed in a thermogravimetric analyzer (TGA, DuPont TGA 51) under a stream of N_2. A 30–50-mg sample was used for each TGA analysis. The sample was heated at 30°C/min from room temperature to maximum heat-treatment temperatures in a range of 700–950°C. The volatile evolution behavior during carbonization was well monitored by the TGA system.

Activation

Following the carbonization process, the char sample was also gasified in the TGA, in a stream of CO_2 at the maximum heat-treatment temperature. External mass-transfer limitations have been determined to be insignificant in the range of reaction rates of interest here; this is confirmed by the fact that the reaction rate was not affected by increasing the gas flow rate at the highest temperature studied. Activated carbons with various degrees of burnoff were prepared.

Table 1. Coal Analysis (wt. %)

Ultimate (dry-ash-free basis)	
Carbon	71
Nitrogen	1.1
Hydrogen	5.7
Oxygen	22
Sulfur	0.13
Proximate (as-received basis)	
Moisture	13
Volatile matters	39
Fixed carbon	46
Ash	1.5

Sample characterization

Specific surface areas and pore volumes of the samples were determined by gas adsorption. An automated adsorption apparatus (Micromeritics, ASAP 2000) was employed for these measurements. Nitrogen adsorption at -196°C and CO_2 adsorption at 0°C were measured. Before any such analysis the sample was degassed at 300°C in a vacuum at about 10^{-3} torr. The N_2 and CO_2 isotherms were analyzed by the BET equation (Gregg and Sing, 1982; Lowell and Shields, 1991) and the Dubinin–Polanyi (DP) equation (Lowell and Shields, 1991), respectively, to determine the surface areas of the chars. Micropore volumes of the samples were determined from the application of the Dubinin–Radushkevich (DR) equations (Stoeckli, 1990) to both of the N_2 and CO_2 adsorption isotherms.

In type I isotherms (Gregg and Sing, 1982; Lowell and Shields, 1991), the amount of N_2 adsorbed at relative pressures near unity corresponds to the total amount adsorbed at both micropores (filled at low relative pressures) and mesopores (filled by capillary condensation at relative pressures above 0.2); and, consequently the subtraction of the N_2 micropore volume (from the DR equation) from the total amount (determined at $p/p_0 = 0.98$ in this case) will provide the volume of the mesopore (Rodriguez-Reinoso et al., 1995). The average pore diameter can be estimated according to the N_2 BET surface area and total pore volume, if the pores are assumed to be parallel and cylindrical.

Results and Discussion

Carbonization results

The results of carbonization performed in TGA under an N_2 environment is shown in Figure 1. It can be seen from the figure that the carbonization process can be approximately described by broad peaks of moisture and volatile matter. Tar is probably a predominant product of devolatilization for a significant part of the process, so that a sharp peak for volatile evolution is observed. The temperature range for the volatile evolution is referred to as offering a clue to the key mechanistic steps in the overall coal breakdown process (Serio et al., 1987). The temperature at which volatile evolution reaches the maximum (peak temperature) during carbonization was determined to be 460°C, which was lower than those for the carbonization of bituminous coals in our previous study (Teng et al., 1996). It has been pointed out that the peak temperature generally decreases with the increase of the O/C atomic ratio of the bituminous coals, since oxygen may play an important role in forming an intermediate structure facilitating volatile escape during carbonization. The coal used in the present study has an O/C atomic ratio of 0.23, which is higher than those of the butiminous coals (in a range of 0.067–0.11). The trend for the variation of the peak temperature with the O/C ratio was still maintained, although a different rank of coal was carbonized in the present study.

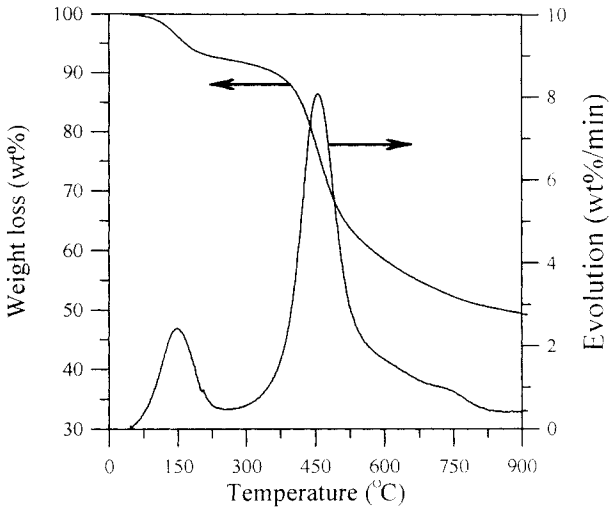

Figure 1. Weight loss and evolution rate during carbonization of the subbituminous coal in N_2.

Wt. % on an as-received basis; heating rate, 30°C/min.

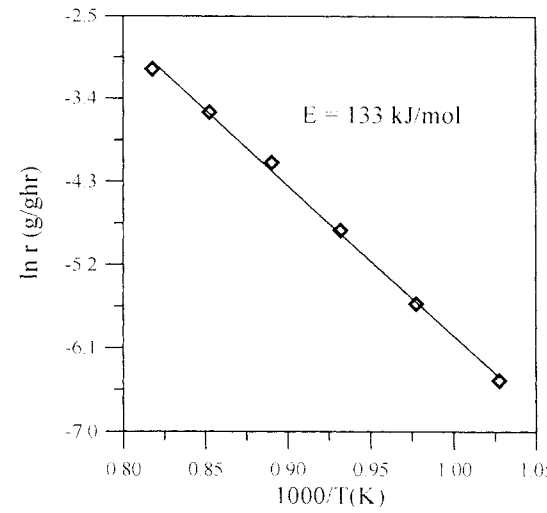

Figure 3. Temperature dependence of the gasification rate (r) in CO_2 at 10% of carbon burnoff.

The experiments were conducted at a CO_2 pressure of 101 kPa.

Global kinetics for CO_2 activation

Following the carbonization of the coal in N_2, the resulting char was subjected to activation, in order to increase the surface area and pore volume of the carbon. The activation was performed by gasifying the char in CO_2 at the maximum heat-treatment temperature. The degree of activation in the present study is therefore represented by the extent of char burnoff in CO_2. During the course of activation, the sample mass was monitored by the TGA, and the rate of activation (or gasification) was determined based on the rate of carbon consumption. Figure 2 shows the rate of activation of the chars at different activation temperatures. The figure reveals how the degree of activation varies with the activation time. The global rate expression for the carbon gasified in CO_2 can be written as

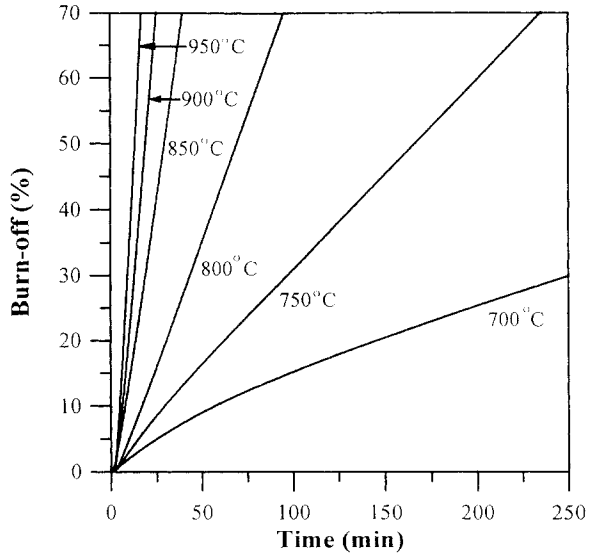

Figure 2. Rate of activaton of the chars at different temperatures in CO_2.

$$r = -dw_c/[(w_c)dt] = A\exp(-E/RT)(P_{CO_2})^n, \quad (1)$$

where r is the global gasification rate per unit mass of carbon; w_c is the mass of carbon; A is the frequency factor; E is the apparent activation energy of gasification; and n is the apparent reaction order with respect to CO_2 partial pressure. According to the results in Figure 2, the gasification rates at various temperatures and extents of burnoff can be determined. An example of the temperature dependence of the gasification rate, obtained at a carbon burnoff of 10%, is shown in Figure 3, an Arrhenius-type plot of $\ln r$ vs. $1/T$, providing an estimate of the gasification activation energy. It appears that, according to Figure 3, the activation energy is a constant over the temperature range employed. The temperature dependence of the reactivity of the char in CO_2 at various extents of burnoff, in a range of 2.5–65%, was also determined, and the results are shown in Figure 4. It can be seen that the activation energy increases with the extent of burnoff, varying within a range of 100–150 kJ/mol.

It is well known that heterogeneous gas–solid reactions involving a single char particle are governed by an intricate coupling of transport phenomena and chemical kinetics (Laurendeau, 1978). There are three ideal zones. Zone I represents the case for which chemical reaction within the particle is slow compared to diffusion, thus allowing an essentially constant reactant concentration across the external gas film and throughout the particle. In zone II the chemical reaction rate has become too great for the reactant concentration within the pore structure to be maintained by diffusion through the pores, and the observed rate is determined by chemical reaction plus internal pore diffusion. The characteristic condition of zone II is for the reactant concentration to be zero at the center of the particle and equal to the bulk concentration at particle surface (Mulcahy and Smith, 1969). In zone III, the chemical reaction within the pore structure is so rapid with respect to diffusion that the reactant gas concentration approaches zero both within and at the particle

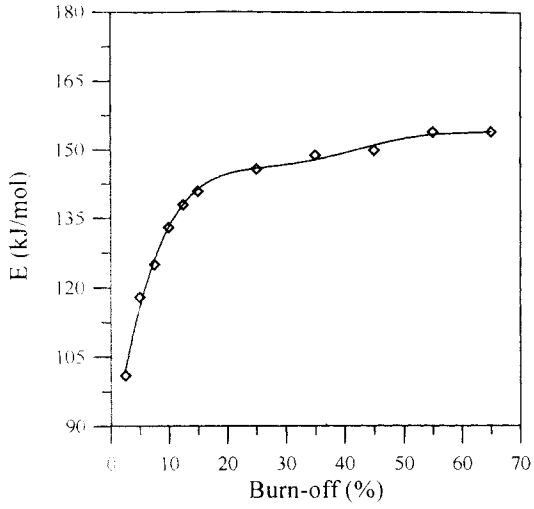

Figure 4. Variation of apparent activation energy with burnoff level for the char gasified in CO_2.

The reaction rates used to calculate the activation energies were determined based on per-unit mass of the carbon.

surface. Thus, the overall reactivity is controlled solely by external film diffusion. In the present study, the external mass-transfer limitations have been determined to be insignificant, and, therefore, only the internal pore diffusion effect has to be considered here. For a carbon gasification that occurs in zone II or in the transition region between zone II and zone I, the apparent activation energy generally increases with a decrease in pore-diffusion resistance (Mulcahy and Smith, 1969; Laurendeau, 1978). Since the apparent activation energy for this gasification varies with the burnoff level of the carbon, it is suspected that the diffusion of CO_2 through the porous structure of the carbon may play an important role in this reaction. An understanding of how the surface characteristics of the carbon vary with the burnoff level is required to clarify this issue. This aspect is discussed further later, along with the development of surface properties with the burnoff level.

Development of surface area and pore volume

Adsorption isotherms of N_2 on the carbons, with different degrees of burnoff in CO_2 at 750 and 900°C, are shown in Figure 5. The isotherms are typical of microporous carbons (type I); that is, the knees of the isotherms are sharp and the plateaus are fairly horizontal (Muñoz-Guillena et al., 1992). The adsorption capacity of the activated carbon increases with the extent of burnoff, indicating the increase of porosity upon activation. It can also be seen that the activated carbons prepared at 750°C are mainly microporous, and as the activation temperature increases to 900°C, there is a widening of the porosity by an increase in supermicroporosity and mesoporosity, as inferred from the opening of the knee of the isotherm and the higher slope of the plateau (Muñoz-Guillena et al., 1992).

The isotherms of the activated carbons prepared from the other temperatures are also typical of microporous carbons and show a similar trend for the influence of the activation temperature. These adsorption data were employed to deter-

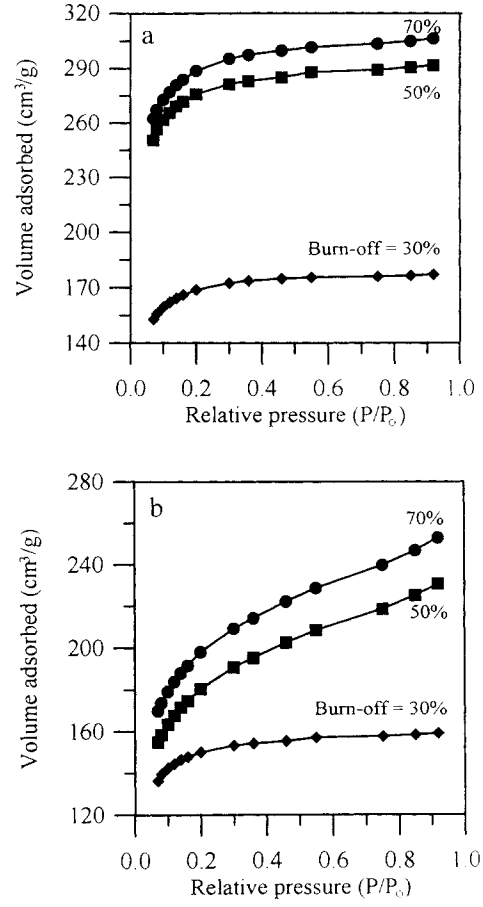

Figure 5. Adsorption isotherms of N_2 on the activated carbons with different degrees of burnoff in CO_2 at (a) 750°C and (b) 900°C.

mine the surface properties of the carbons. The developments of the surface area, pore volume, pore-size distribution, and average pore diameter as functions of the burnoff level for carbons activated at different temperatures are shown in Table 2. One can observe from Table 2 that the surface area and pore volume of the carbons prepared at different temperatures unanimously increase upon activation, as indicated from the adsorption isotherms shown in Figure 5. The proportion of mesopore volume and the average pore diameter generally increases with the burnoff level, showing the enlarging of micropores upon activation. Decreases in pore volume and surface area upon activation were observed at high extents of carbon burnoff in our previous studies (Teng et al., 1996, 1997). This was attributed to the fact that, at high levels of burnoff, pore walls break to decrease the surface area and exterior carbons gasify to eliminate the pores. No decrease in surface area and pore volume with burnoff level was observed in the present study, suggesting that gasification mainly occurs at the interior of the carbon particles to increase the pore volume and surface area.

As for the effect of activation temperature, it can be seen from Table 2 that the surface area and pore volume pass through a maximum at an activation temperature of 750°C. The increase in porosity when the preparation temperature is raised from 700°C to 750°C can be attributed to the release

Table 2. Surface Characteristics (N_2 Adsorption) vs. Extent of Burnoff for Activated Carbons at Different Activation Temperatures

Burnoff (%)	BET S.A. (m^2/g)	Pore Vol. (cm^3/g)	Pore-Size Distribution		Avg. Pore Dia. (Å)
			Micro (%)	Meso (%)	
700°C Activation					
0	5.39	ND*	ND	ND	ND
30	542	0.263	98	2	19.2
50	791	0.387	97	3	19.6
70	893	0.469	95	5	19.9
750°C Activation					
0	1.66	ND	ND	ND	ND
30	579	0.278	99	1	19.4
50	944	0.458	98	2	19.6
70	988	0.482	97	3	19.9
800°C Activation					
0	19.8	0.007	ND	ND	ND
30	543	0.258	100	0	19.5
50	783	0.383	97	3	19.7
70	836	0.400	96	4	19.9
850°C Activation					
0	3.89	ND	ND	ND	ND
30	530	0.254	99	1	19.6
50	629	0.320	93	7	20.1
70	730	0.352	96	1	20.3
900°C Activation					
0	0.87	ND	ND	ND	ND
30	507	0.250	96	4	19.7
50	596	0.394	72	28	23.4
70	713	0.413	79	21	23.8
950°C Activation					
0	17.0	0.038	ND	ND	ND
30	453	0.247	87	13	21.8
50	554	0.287	92	8	20.8
70	611	0.360	81	19	24.1

*Not detectable.

of tars blocking the entrances of micropores generated during carbonization (Ibarra et al., 1991). For preparation temperatures above 750°C, the surface area and pore volume decrease with the temperature. The development of surface area and pore volume is related to the formation of cross-links between carbonaceous aggregates. Therefore, at higher temperatures it is demonstrated that the cross-links break, with a consequent rearrangement of carbonaceous aggregates and the collapse of pores, which render most of the porosity inaccessible to nitrogen at −196°C (Alvarez et al., 1992; Jagtoyen and Derbyshire, 1993).

The variation in activation temperature affects not only the specific pore volume of the resulting carbons, but also the pore size. It can be observed that the average pore diameter calculated from the surface area and pore volume increases as the activation temperature is elevated. Similar results have been reported by other studies (Kovacik et al., 1995; Teng et al., 1996) in the preparation of activated carbon. The transport phenomena during the course of carbon gasification may explain the results. At high temperatures the chemical reaction between CO_2 and carbon atoms is so fast that CO_2 diffusion in pores becomes the slow step; therefore, most of the gasification occurs on the pore walls close to the pore entrance before CO_2 molecules diffuse to the innermost of the pores, and, thus, pore widening happens. On the other hand, since the rates of diffusion and chemical reaction are comparable at low temperatures, the CO_2 molecules are able to diffuse inside and to react with the carbon atoms on the deeper portion of the pore walls, which results in pore deepening. The increase in mean pore size with the activation temperature found in the present study may thus be attributed to the fact that pore widening is the predominant mechanism at high temperatures due to a strong pore resistance, whereas pore deepening is favored by low temperatures because of the relatively rapid diffusion of CO_2 into the pores.

It would be worthwhile to note that the carbons activated at temperatures lower than 900°C are mainly microporous, as shown in Table 2, whereas the proportion of mesoporosity becomes nonnegligible (> 10%) for carbons prepared at temperatures above 900°C. The results from the present study show that pore structure development can be well tailored not only by controlling the degree of activation, but also by varying the activation temperature.

The results in Table 2 show that the N_2 BET surface area of the char obtained from carbonization is small initially and increases enormously after burnoff in CO_2. It has been stated that this might be an artifact because of activated diffusion of N_2 at −196°C (Ballal and Zygourakis, 1987; Su and Perlmutter, 1985), and is quickly removed after some carbon burnoff. To clarify the facts of this aspect, CO_2 adsorption on the activated carbons at 0°C were measured, and, as stated in the Experimental Section, the isotherms were analyzed by the DP and the DR equations (Lowell and Shields, 1991) to determine the surface area and the micropore volume, respectively, of the carbons.

The results of surface analysis determined by CO_2 adsorption are shown in Table 3. Comparing Table 3 with the results in Table 2 reveals that the varieties of surface characteristics determined by CO_2 are similar to those determined by N_2 adsorption; that is, the surface area and pore volume of the activated carbon increase with the degree of burnoff in CO_2 for each activation temperature, and pass through a maximum at an activation temperature of 750°C for the carbons of the same burnoff level. However, the surface area and pore volume of the 0% burnoff carbons determined by CO_2 adsorption are much higher than those determined by N_2 adsorption. This difference is certainly due to the effect of the activated diffusion of N_2 at −196°C, and is usually observed for activated carbons with small degrees of burnoff (Garrido et al., 1987). The most important factor in greater uptake of CO_2 is the higher temperature of adsorption, which allows the molecules to overcome the energy barrier at the pore entrance (Sing, 1989).

Micropore volume deduced from the application of the DR equation to the isotherms of N_2 at −196°C provides the volume of the micropores, including the so-called supermicropores (Rodríguez-Reinoso et al., 1995), whereas the value determined from the isotherm of CO_2 at 0°C corresponds to the volume of narrow micropores (up to about 0.7 nm). Using both N_2 and CO_2 adsorption isotherms can provide useful information concerning the micropore size distribution (Garrido et al., 1987). The fact that the amount of CO_2 adsorption rate on the 0% burnoff carbons at 0°C is greater than that of N_2 at −196°C reveals that the microporosity is very narrow for low burnoff carbons. For the carbons with a burnoff level above 30%, the amount of N_2 adsorption is

Table 3. Surface Characteristics (CO_2 Adsorption) vs. Extent of Burnoff for Activated Carbon at Different Activation Temperatures

Burnoff (%)	DP S.A. (m^2/g)	DR Vol. (CO_2) (cm^3/g)
700°C Activation		
0	455	0.170
30	565	0.212
50	650	0.229
70	773	0.290
750°C Activation		
0	456	0.171
30	647	0.242
50	714	0.268
70	754	0.283
800°C Activation		
0	435	0.163
30	592	0.221
50	683	0.256
70	719	0.269
850°C Activation		
0	420	0.157
30	561	0.210
50	632	0.237
70	702	0.263
900°C Activation		
0	268	0.100
30	531	0.199
50	572	0.214
70	656	0.246
950°C Activation		
0	165	0.088
30	484	0.181
50	551	0.206
70	593	0.222

larger than that of CO_2, indicating that there is no problem of restricted diffusion of N_2 at -196°C and that the microporosity is wide and heterogeneous. Also, according to the data in Tables 2 and 3, the differences in the amounts of N_2 and CO_2 adsorptions increase with the extent of burnoff, indicating that microporosity becomes wider upon activation. This is in agreement with the previous finding that the average pore diameter increases with the extent of burnoff.

The preceding results reveal that even under a similar degree of burnoff the carbons prepared from different temperatures exhibit different surface characteristics. Assuming that the surface is fully accessible and has a uniform reactivity, the rate of gasification would be proportional to the surface area of the carbon. Under this circumstance, the gasification rate in terms of per unit total surface area (TSA), which equals r/TSA, should be the value employed in the analysis of the reaction kinetics. The quantity r is the pseudosteady mass loss rate per unit mass in CO_2 at the indicated gasification temperature. Here TSA represents the larger of the N_2 BET and CO_2 DP surface areas. An example of temperature dependence of r/TSA is shown in Figure 6. The activation energy determined from Figure 6 appears to be larger than that from Figure 3, which is also the case for other burnoff levels. The variation in the apparent activation energy with the degree of burnoff is shown in Figure 7. Similar to the results shown in Figure 4, the apparent activation energy, E', based on the uniform surface assumption, increases with the degree of burnoff, varying within a range of 130–180 kJ/mol.

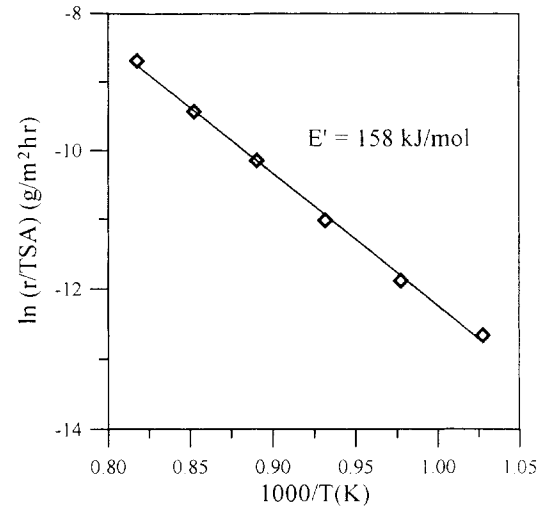

Figure 6. Temperature dependence of the gasification rate (r/TSA) in CO_2 at 10% of carbon burnoff.

The experiments were conducted at a CO_2 pressure of 101 kPa.

The results in Figure 7 further support the earlier inference that the diffusion resistance of CO_2 through the porous structure of the carbon may play an important role in this reaction. An increase in pore size may result in a decrease in pore diffusion resistance. Thus, the increase in the activation energy with the burnoff level implies that the pores are widened upon gasification to reduce the diffusion resistance. The data in Table 2 indeed show that the average pore diameter increases upon gasification, which may explain why the apparent activation energy increases with the degree of burnoff. Therefore, it is firmly believed that the carbon gasification occurs in zone II or in the transition region between zone II and zone I.

A cylindrical pore model has been applied to evaluate the effectiveness factor for this reaction at different extents of

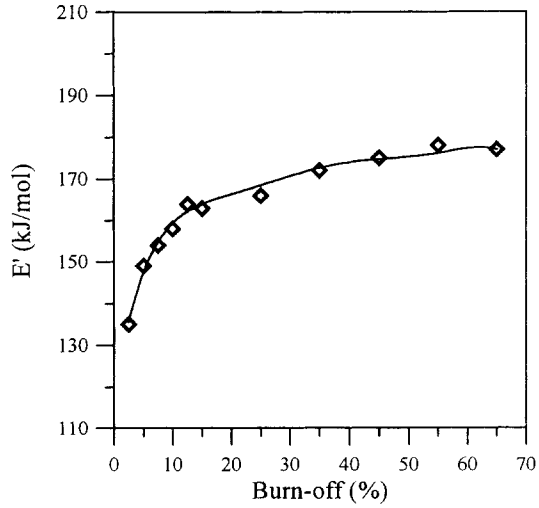

Figure 7. Variation of apparent activation energy with burnoff level for the char gasified in CO_2.

The reaction rates used to calculate the activation energies were determined based on per-unit total surface area of the carbon.

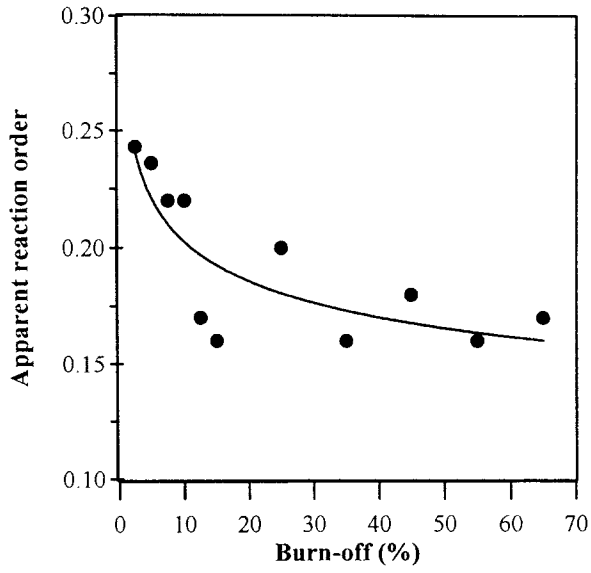

Figure 8. Variation of apparent reaction order with the extent of burnoff in CO_2 at 800°C.

burnoff. However, the evaluation cannot precisely predict the variation of the apparent activation energy with the burnoff level, as shown in the present study. Obviously, a more sophisticated pore model is required to interpret the variation of the activation energy with the burnoff level.

The apparent reaction order with respect to CO_2 partial pressure for this activation, n, was also determined. In order to determine this kinetic parameter, the gasification of the carbonized samples was performed under different CO_2 pressures, varying in a range of 50.7–101 kPa. Using the experimental results, the apparent orders at various degrees of burnoff and different activation temperatures were calculated. Figure 8 shows an example of the variation of the apparent order with the burnoff level at an activation temperature of 800°C. The results for the activation at the other temperatures are similar to that shown in Figure 8. It can be seen that the reaction orders are low, varying in a range of 0.15–0.25. The figure apparently shows a decrease in the apparent order with the burnoff level. This finding can be, at least partially, attributed to the influence of pore resistance, according to the following qualitative discussion. For a reaction with the intrusion of pore diffusion resistance, the apparent order of the reaction should exhibit a value between m and $(m+1)/2$, where m is the intrinsic order for the reaction occurring in zone I (Mulcahy and Smith, 1969; Laurendeau, 1978). Under this circumstance, the apparent order would increase with the increase in pore resistance for a reaction with its intrinsic order less than unity. At lower degrees of burnoff (narrow microporosity), the intrusion of pore-diffusion resistance is enhanced, resulting in an increase in the apparent reaction order, as observed in Figure 8.

Conclusions

This study has demonstrated that high-porosity activated carbon can be prepared from a low-ash subbituminous coal through the physical activation by CO_2. The surface area and the pore volume of the carbon produced can be as high as 1000 m^2/g and 0.48 cm^3/g, respectively.

During the course of carbonization, the release of moisture and tar represented most of the evolution. The porosity of the resulting carbons determined by N_2 adsorption at −196°C was much lower than that by CO_2 at 0°C, indicating a narrow microporosity of the carbon.

Activated carbons with various degrees of burnoff were prepared, and the adsorption results revealed that the carbons were mainly microporous. The surface area and pore volume of the carbons both increased with the extent of carbon burnoff for each activation temperature. The average pore diameter also generally increased upon activation.

The surface characteristics of the activated carbons were influenced by the activation temperature. The surface area and pore volume pass through a maximum at an activation temperature of 750°C; these values increased by raising the temperature from 700°C to 750°C, and decreased with the temperature while above 750°C.

The activation energy for the gasification of the carbon in CO_2 was found to be in the range of either 100–150 kJ/mol or 130–180 kJ/mol, under the assumption that the gasification rate was proportional to the carbon mass or the total surface area, respectively. The activation energy increased with the burnoff level, and this was attributed to the reduced intrusion of the pore diffusion resistance, caused by the widening of the pores upon activation. The apparent reaction order with respect to the CO_2 partial pressure was low, in a range of 0.15–0.25.

The results of the present study show that pore structure development during the course of activated carbon preparation can be tailored by controlling the degree of activation as well as the activation temperature.

Acknowledgment

This research was supported by the National Science Council of Taiwan, through Project NSC 87-2214-E-006-038.

Literature Cited

Ahmadpour, A., and D. D. Do, "The Preparation of Active Carbons from Coal by Chemical and Physical Activation," *Carbon*, **34**, 471 (1996).

Ahmadpour, A., and D. D. Do, "Characterization of Modified Activated Carbons: Equilibria and Dynamics Studies," *Carbon*, **33**, 1393 (1995).

Alvarez, T., A. B. Fuertes, J. J. Pis, J. B. Parra, J. Pajares, and R. Menéndez, "Influence of Coal Oxidation on the Structure of Char," *Fuel*, **73**, 1358 (1994).

Bansal, R. C., J. B. Donnet, and H. F. Stoekcli, *Active Carbon*, Dekker, New York (1988).

Ballal, G., and K. Zygourakis, "Evolution of Pore Surface Area during Noncatalytic Gas-Solid Reactions: 2. Experimental Results and Model Validation," *Ind. Eng. Chem. Res.*, **26**, 1787 (1987).

Cooney, D. O., *Activated Charcoal*, Dekker, New York (1980).

Garrido, J., A. Linares-Solano, J. M. Martín-Martínez, M. Molina-Sabio, F. Rodríguez-Reinoso, and R. Torregrosa, "Use of N_2 vs. CO_2 in the Characterization of Activated Carbons," *Langmuir*, **3**, 76 (1987).

Greenbank, M., and S. Spotts, "Six Criteria for Coal-Based Carbons," *Water Technol.*, **16**, 56 (1993).

Gregg, S. J., and K. S. W. Sing, *Adsorption, Surface and Porosity*, Academic Press, London (1982).

Ibarra, J. V., R. Moliner, and J. M. Palacios, "Catalytic Effects of Zinc Chloride in the Pyrolysis of Spanish High Sulphur Coals," *Fuel*, **70**, 727 (1991).

Jagtoyen, M., and F. Derbyshire, "Some Considerations of the Origins of Porosity in Carbons from Chemically Activated Wood," *Carbon*, **32**, 1185 (1993).
Kovacik, G., B. Wong, and E. Furimsky, "Preparation of Activated Carbon from Western Canadian High Rank Coals," *Fuel Proc. Technol.*, **41**, 89 (1995).
Laine, J., and S. Yunes, "Effect of the Preparation Method on the Pore Size Distribution of Activated Carbon from Coconut Shell," *Carbon*, **30**, 601 (1992).
Laurendeau, N. M., "Heterogeneous Kinetics of Coal Char Gasification and Combustion," *Prog. Energy Comb. Sci.*, **4**, 221 (1978).
Lowell, S., and J. E. Shields, *Powder Surface Area and Porosity*, 3rd ed., Chapman & Hall, London (1991).
Lu, G. Q., "Evolution of Pore Structure of High-Ash Char During Activation," *Fuel*, **73**, 145 (1994).
Mulcahy, M. F. R., and I. W. Smith, "Kinetics of Combustion of Pulverized Fuel: A Review of Theory and Experiment," *Rev. Pure Appl. Chem.*, **19**, 81 (1969).
Muñoz-Guillena, M. J., M. J. Illán-Gómez, J. M. Martín-Martínez, A. Linares-Solano, and C. Salinas-Martínez de Lecea, "Activated Carbons from Spanish Coal: I. Two-Stage CO_2 Activation," *Energy Fuels*, **6**, 9 (1992).
Rodríguez-Reinoso, F., M. Molina-Sabio, and M. T. González, "The Use of Steam and CO_2 as Activating Agents in the Preparation of Activated Carbons," *Carbon*, **33**, 15 (1995).
Serio, M. A., D. G. Hamblen, J. R. Markham, and P. R. Solomon, "Kinetics of Volatile Product Evolution in Coal Pyrolysis: Experiment and Theory," *Energy Fuels*, **1**, 138 (1987).
Sing, K. S. W., "The Use of Physisorption for the Characterization of Microporous Carbons," *Carbon*, **27**, 5 (1989).
Stoeckli, H. F., "Microporous Carbons and Their Characterization: The Present State of the Art," *Carbon*, **28**, 1 (1990).
Su, J.-L., and D. D. Perlmutter, "Effect of Pore Structure on Char Oxidation Kinetics," *AIChE J.*, **31**, 973 (1985).
Teng, H., J.-A. Ho, and Y.-F. Hsu, "Preparation of Activated Carbons from Bituminous Coals with CO_2 Activation—Influence of Coal Oxidation," *Carbon*, **35**, 275 (1997).
Teng, H., J.-A., Ho, Y.-F. Hsu, and C.-T. Hsieh, "Preparation of Activated Carbons from Bituminous Coals with CO_2 Activation: 1. Effects of Oxygen Content in Raw Coals," *Ind. Eng. Chem. Res.*, **35**, 4043 (1996).
Wigmans, T., "Industrial Aspects of Production and Use of Activated Carbons," *Carbon*, **27**, 13 (1989).

Manuscript received Sept. 19, 1997, and revision received Feb. 9, 1998.